PAPER

Dynamics of a Floating Platform Mounting a Hydrokinetic Turbine

AUTHORS

Tobias Dewhurst
M. Robinson Swift
Martin Wosnik
Kenneth Baldwin
Judson DeCew
Matthew Rowell
Center for Ocean Renewable Energy, University of New Hampshire

ABSTRACT

A two-dimensional mathematical model was developed to predict the dynamic response of a moored, floating platform mounting a tidal turbine in current and waves. The model calculates heave, pitch, and surge response to collinear waves and current. Waves may be single frequency or a random sea with a specified spectrum. The mooring consists of a fixed anchor, heavy chain (forming a catenary), a lightweight elastic line, and a mooring ball tethered to the platform. The equations of motion and mooring equations are solved using a marching solution approach implemented using MATLAB. The model was applied to a 10.7-m twin-hulled platform used to deploy a 0.86-m shrouded, in-line horizontal axis turbine. Added mass and damping coefficients were obtained empirically using a 1/9 scale physical model in tank experiments. Full-scale tests were used to specify drag coefficients for the turbine and platform. The computer model was then used to calculate full-scale mooring loads, turbine forces, and platform motion in preparation for a full-scale test of the tidal turbine in Muskeget Channel, Massachusetts, which runs north-south between Martha's Vineyard and Nantucket Island. During the field experiments, wave, current, and platform motion were recorded. The field measurements were used to compute response amplitude operators (RAOs), essentially normalized amplitudes or frequency responses for heave, pitch, and surge. The measured RAOs were compared with those calculated using the model. The very good agreement indicates that the model can serve as a useful design tool for larger test and commercial platforms.

Keywords: tidal energy, floating platform dynamics, seakeeping, Muskeget Channel, wave response field measurements

Introduction

Floating platforms have been used to test and demonstrate the use of hydrokinetic turbines in tidal currents. Examples include Verdant Power's (2005) deployment of a Gorlov turbine in the tidal Merrimack River, Ocean Renewable Power Company's (Hewitt, 2010) barge demonstration of their turbine in Cobscook Bay and the performance evaluation of tidal turbines in the Piscataqua River, New Hampshire, and Muskeget Channel, Massachusetts (Rowell, 2013). In the last two applications, the floating platform made use of a twin-hulled, decked configuration having a derrick built around a central opening for raising and lowering the turbine. The platform was anchored in place during actual testing as shown in the Figure 1 schematic. The convenience and cost effectiveness of this concept has resulted in the design of larger, more capable platforms (Byrne, 2011, 2013). In addition, several developers of commercial systems have noted that floating tidal energy platforms have significantly lower installation and maintenance costs compared to fixed, bottom-mounted systems (see, e.g., Francis & Hamilton, 2007).

Floating platforms, however, are limited by stability in strong currents and sea-keeping response to waves in exposed sites. The drag force acting on a turbine mounted below the hull can generate a bow-down tipping moment, reducing freeboard. The downward pull of the bow anchor line also contributes to bow-down tipping moment unless a large float is used, which may disturb the incident flow. In addition, waves can cause unsafe conditions, such as excessive water-on-deck or waves impacting the underside of the deck. Waves may also limit operations, causing crew discomfort to the extent that they may be incapacitated (see, e.g., Sarioz & Narli, 2005).

To determine the behavior of the platform in current and waves, a two-dimensional mathematical model of the platform-turbine-mooring system was developed. The model predicts the horizontal displacement (surge), rotation angle (pitch), and vertical displacement (heave) response to collinear waves and current. Waves may be single frequency or a random sea with a specified spectrum. This model

FIGURE 1

Floating platform anchored in tidal current with turbine mounted below. Mooring can be single-point or fore and aft (not shown).

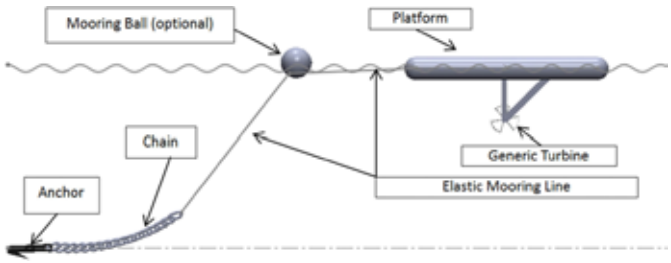

differs significantly from traditional sea-keeping models (e.g., Salvesen et al., 1970) because of nonlinear drag forces on the turbine and platform including mounting structure and the presence of a mooring system. The mooring consists of a fixed anchor, heavy chain (forming a catenary), and a lightweight elastic line extending to a mooring ball and then to the platform.

In this paper, the heave, pitch, and surge equations of motion, along with the mooring system equations, are developed. The complete set of dynamic equations was solved using a "marching solution" approach implemented in MATLAB. The results of single frequency wave excitation were used to find response amplitude operators (RAOs), which can be used to characterize sea-keeping response (St. Denis & Pierson, 1953). The model was applied to the University of New Hampshire (UNH) 10.7-m (35-foot) tidal energy test platform that was deployed during Summer 2012 in the exposed Muskeget Channel, Massachusetts, and subject to waves and current while testing a shrouded tidal turbine. Damping and inertial coefficients were found using a 1/9 scale physical model in wave/tow tank experiments. Drag coefficients were found from full-scale experiments. Initial comparisons between model predictions and wave tank data justified using the mathematical model to design the mooring system, compute fluid dynamic loads on the turbine, and identify operating limits of the platform in preparation for the field deployment. During the field experiments, platform motion, wave surface elevation, and current were measured. This data set was used to validate the model under full-scale field conditions.

Heave-Pitch-Surge Model

The mathematical model was developed directly from the component equations of motion incorporating a nonlinear (velocity squared) representation for drag forces, including the important drag of the turbine, as well as nonlinear relations describing the mooring system. Because of this mathematical complexity, a first principles approach was chosen rather than adapt the standard linear sea-keeping methods for unmoored surface vessels described by, for example, the Society of Naval Architects and Marine Engineers (1988) and Faltinsen (1990). Nevertheless, the nomenclature used here for position variables and linear restoring and wave excitation coefficients is consistent with standard sea-keeping analysis.

The forces and moments acting directly on the platform are shown on the Figure 2 free body diagram.

From Figure 2, Newton's second law applied in the horizontal (surge, subscript 1, or x-direction) yields the following equation of motion:

$$F_{Dp1} + F_{Dt} + F_{Ap1} + F_{At} - F_{Tl}\cos\phi = \ddot{\eta}_1 m. \quad (1)$$

Here F_{Dp1} is the drag force on the platform, F_{Dt} is the drag force on the turbine, F_{Ap1} is the fluid acceleration force on the platform, F_{At} is the fluid acceleration force on the turbine, and F_{Tl} is the mooring line tension. Furthermore, $\ddot{\eta}_1$ is the acceleration of the platform in surge and m is the mass of the system. The drag forces on the device and support structure, which generally involve bluff body

FIGURE 2

Free-body diagram of surface platform with wave and current forcing.

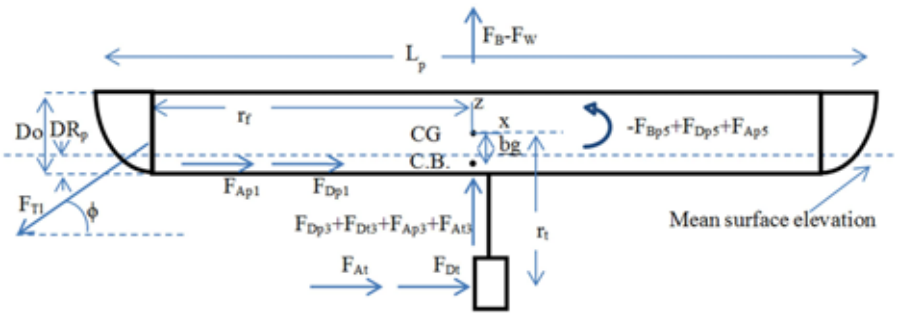

components, are taken to be proportional to the square of relative fluid velocity, so the general drag force representation has the form

$$F_D = \frac{1}{2} C_D \rho A U |U| \tag{2}$$

where C_D is a drag coefficient, ρ is fluid density, A is projected area, and U is the relative fluid velocity.

The equation of motion in the vertical (heave, subscript 3, or z-direction) is

$$F_{Bp} + F_{Bt} - F_{Wp} - F_{Wt} + F_{Dp3} + F_{Dt3} + F_{Ap3} + F_{Apt} - F_{Tl}\sin\phi = \ddot{\eta}_3 m. \tag{3}$$

Here F_{Bp} and F_{Bt} are the buoyant force on the platform and turbine, respectively; F_{Wp} and F_{Wt} are the weight of the platform and turbine, respectively; F_{Dp3} and F_{Dt3} are the heave damping force on the platform, turbine (including wave and viscous damping); and F_{Ap3} and F_{At3} are the heave added mass force on the platform and turbine, respectively. Furthermore, $\ddot{\eta}_3$ is the acceleration of the platform in heave.

Consideration of moments about the negative y-axis passing through the center of gravity (CG), associated with pitch or subscript 5 rotation, results in

$$-F_{Bp5} + F_{Dp5} + F_{Ap5} + (F_{At} + F_{Dt}) r_t + r_f F_{Tl}\sin\phi = \ddot{\eta}_5 I_5. \tag{4}$$

Here F_{Bp5} is the buoyancy moment applied to the platform, F_{Dp5} is the damping moment applied to the platform, F_{Ap5} is the added mass moment applied to the platform, r_t is the vertical distance from the center of gravity to the turbine hub, and r_f is the horizontal distance from the center of gravity to the mooring attachment point. Furthermore, $\ddot{\eta}_5$ is the angular acceleration of the platform in pitch, and I_5 is the mass moment of inertia of the system about the y-axis.

Buoyancy Forces

For equilibrium conditions with no current, the total buoyancy force in the heave direction, $F_{Bp} + F_{Bt} = F_B$, is equal to the weight of the system, $mg = F_W = F_{Wp} + F_{Wt}$. When the water level changes relative to the system's center of gravity, CG, an incremental change in the buoyant force is induced so that the total buoyant force minus weight in heave can be written as

$$F_{Bp} + F_{Bt} - F_{Wp} - F_{Wt} = F_B - mg = \rho g A_{wp} \left(\zeta_{3eff} - \eta_3 \right) \tag{5}$$

where m is the mass of the system, η_3 is the heave displacement of the system, A_{wp} is the planform area of the platform at the waterline, and ζ_{3eff} is the surface elevation averaged over length L of the platform. For a linear surface wave, this is

$$\begin{aligned} \zeta_{3eff} &= \frac{1}{L} \int_{-\frac{L}{2}+\eta_1}^{\frac{L}{2}+\eta_1} \frac{H}{2} \cos(kx - \sigma_e t) dx \\ &= \frac{\sin\left(\frac{kL}{2}\right)}{\frac{kL}{2}} \frac{H}{2} \cos(k\eta_1 - \sigma_e t) \end{aligned} \tag{6}$$

where $k = 2\pi/\lambda$ is the wave number; λ is wavelength, σ_e is the wave radian encounter frequency (wave frequency modified by advection of the wave field at the current velocity), H is wave height, and η_1 is platform surge displacement. The hydrostatic

moment on the platform is the sum of the hydrostatic restoring moment and the wave forcing moment. Thus, the buoyancy moment is

$$F_{Bb5} = (mg)\overline{gm}(-\eta_5) + \int_A \rho g \zeta_3(x) x dx \tag{7}$$

where the product mg is the buoyant force, $\overline{gm}$ is the metacentric height, η_5 is the pitch angle, and ζ_3 is the surface elevation. (This equation approximates the instantaneous buoyant force with the equilibrium buoyant force, mg, and based on the slender pontoons being nearly symmetrical fore-and-aft, the buoyancy moment due to heave displacement was neglected.) Substituting in for surface elevation from linear wave theory yields

$$F_{Bb5} = (mg)\overline{gm}(-\eta_5) + \int_{-\frac{L}{2}+\eta_1}^{\frac{L}{2}+\eta_1} \rho g H \cos(kx + k\eta_1 - \sigma_e t) x b dx. \tag{8}$$

Here the planform area of the platform at the waterplane is treated as a rectangle of length L and constant width b. The result of this integration can be shown to be

$$F_{Bb5} = (mg)\overline{gm}(-\eta_5) + \rho g b \left[-\frac{L\cos\left(\frac{kL}{2}\right)}{k} + \frac{2\sin\left(\frac{kL}{2}\right)}{k^2} \right] \frac{H}{2} \sin(\sigma_e t - k\eta_1) + \rho g b \left[\eta_1 L \frac{\sin\frac{kL}{2}}{\frac{kL}{2}} \right] \frac{H}{2} \cos(k\eta_1 - \sigma_e t). \tag{9}$$

Drag and Damping Forces

Horizontal forces on the platform and turbine associated with relative fluid velocity are taken to be proportional to the square of velocity (see Equation 2), in keeping with the dimensional analysis approach to drag forces. In the vertical (heave) direction, however, velocity-dependent forcing is taken to be proportional to the velocity, as in the traditional wave and viscous damping approach common to basic sea-keeping methods. In the pitch mode, a mix of linear and nonlinear contributions is used.

The drag forces in surge are drag on the turbine,

$$F_{Dt} = \frac{1}{2} \rho C_{Dt} A_t U_{hub} |U_{hub}| \tag{10}$$

and drag on the platform,

$$F_{Dp} = \frac{1}{2} \rho C_{Dp} A_p U_{surf} |U_{surf}|. \tag{11}$$

Here the A_t and A_p are the submerged projected areas of the turbine and platform, respectively. The drag coefficients, C_{Dt} and C_{Dp}, are determined experimentally. Relative fluid velocity at the hub is

$$U_{hub} = \left(U_{cur} + \dot{\zeta}_1 - \dot{\eta}_1 - r_t \dot{\eta}_5 \right) \tag{12}$$

at the surface,

$$U_{surf} = \left(U_{cur} + \dot{\zeta}_1 - \dot{\eta}_1 \right) \tag{13}$$

where U_{cur} is the current velocity and $\dot{\zeta}_1$ is the wave-induced fluid velocity, calculated at the appropriate depth using linear wave theory.

In heave, the damping forces are taken to be linear, so those due to the wave velocities and platform velocities can be summed such that

$$F_{D3} = B^*_{p33}\dot{\zeta}_{3eff} - B_{p33}\,\dot{\eta}_3 + B^*_{t33}\dot{\zeta}_3 - B_{t33}\,\dot{\eta}_3 \tag{14}$$

where B_p refers to damping coefficients for the platform, and B_t refers to damping coefficients for the turbine; all were determined experimentally. Here B refers to damping coefficients for motion in still water and B^* refers to damping coefficients for fluid motion past the stationary body. In this model the still water damping coefficient in heave, B_{33}, is assumed to be equal to the wave velocity damping coefficient in heave, B^*_{33}. This approach is comparable to that taken by Korvin-Kroukovsky and Jacobs (1957) and Salvesen et al. (1970). Also, the vertical wave fluid velocity, $\dot{\zeta}_3$, is calculated at the turbine hub depth using linear wave theory and $\dot{\zeta}_{3eff}$ is the vertical fluid velocity at the surface averaged over the length of the platform. The derivation of this is similar to that of the average surface elevation, and the result is

$$\dot{\zeta}_{3eff} = \frac{\sin\left(\frac{kL}{2}\right)}{\left(\frac{kL}{2}\right)}\dot{\zeta}_3. \tag{15}$$

In this case, $\dot{\zeta}_3$ is evaluated at the surface. Since there is no significant wave-induced angular velocity in the fluid (linear wave theory is irrotational), the damping moment applied to the platform in pitch is simply

$$F_{Dp5} = B_{p55}\,\dot{\eta}_5 \tag{16}$$

where B_{p55} is the damping coefficient in pitch and $\dot{\eta}_5$ is the angular velocity of the platform. The turbine's contribution to the drag/damping pitch moment can be simplified by assuming that the pitching of the platform has a negligible effect on the drag/thrust coefficient of the turbine, as demonstrated by Bahaj et al. (2006). Thus, that contribution is

$$F_{Dt5} = F_{Dt}r_t \tag{17}$$

where r_t is the distance from the system's center of gravity to the turbine hub and, again, F_{Dt} is the drag force on the turbine in surge.

Acceleration Forces

The horizontal force on the platform associated with platform and fluid acceleration, F_{Ap1}, is defined as

$$F_{Ap1} = A^*_{p11}\ddot{\zeta}_1 - A_{p11}\,\ddot{\eta}_1 \tag{18}$$

where, as with B, A is the matrix of added mass coefficients for motion in still water; A^* is the added mass coefficient matrix for fluid motion past the stationary body; $\ddot{\zeta}_1$ is the horizontal fluid acceleration; and $\ddot{\eta}_1$ is the platform acceleration in surge. According to Berteaux (1991), A and A^* are related by

$$A^* = A + m. \tag{19}$$

The horizontal acceleration force on the turbine takes a similar form to that on the platform. If the turbine is modeled as a flat plate, m, the mass of the fluid displaced by the body is zero, so $A^* = A$ and the force is

$$F_{At} = A_{t11}\left(\ddot{\zeta}_1 - \ddot{\eta}_1\right) \tag{20}$$

where the added mass is a function of the turbine diameter,

$$A_{t11} = \frac{8}{3}\rho\pi {L_{Dt}}^3. \tag{21}$$

Here L_{Dt} is the diameter of the turbine. In the vertical direction, the same method can be used. Thus, the acceleration force is

$$F_{A3} = A^*_{33}\ddot{\zeta}_{3eff} - A_{33}\,\ddot{\eta}_3. \tag{22}$$

Here, again, $\ddot{\zeta}_3$ is the wave fluid acceleration in the vertical direction, averaged over the length of the platform, and $\ddot{\eta}_3$ is the platform acceleration in heave. Furthermore, A_{33} is the added mass of the system when heaving in still water.

Mooring Forces

The mooring system modeled includes an embedment anchor (assumed fixed), a length of heavy chain, and a fiber rope extending to a mooring ball and then to the platform (see Figure 3). In this model, the primary forces are assumed to be weight and tension. Fluid forces on the line and chain, the weight of the line, and the inertia of the mooring system are neglected. Thus, the line is assumed to always be straight (but elasticity is

FIGURE 3

Catenary mooring system, with mooring ball, in equilibrium.

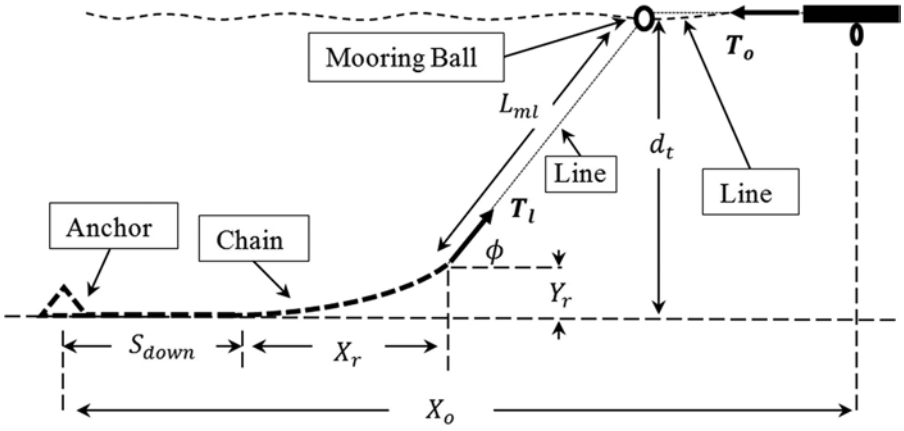

included) and the mooring forces are governed by the catenary equations.

If some chain lies on the seafloor and the line is attached to the platform at the waterline, Berteaux (1991) derives the following governing equations:

$$T_0 = T_l \cos(\phi) \tag{23}$$

$$T_l = T_0 \cosh\left(\frac{pX_r}{T_0}\right) \tag{24}$$

$$d_t = Y_r + L_{ml}\sin(\phi) \tag{25}$$

$$Y_r = \frac{T_0}{p}\left(\cosh\left(\frac{pX_r}{T_0}\right) - 1\right) \tag{26}$$

$$S_{up} = \frac{T_0}{p}\sinh\left(\frac{pX_r}{T_0}\right). \tag{27}$$

The vertical distance d_t is from the ocean bottom to the mooring ball attachment point. Mooring ball inertia is neglected, so that the vertical components of line tensions are in equilibrium with buoyancy force minus ball weight, and the difference in horizontal components of line tensions account for buoy drag calculated using a drag coefficient approach (see Equation 2). If no mooring ball is used, d_t is the vertical distance to the mooring line's attachment point on the platform.

Allowing for elasticity in the straight mooring line introduces the additional equation,

$$L_{ml} = L_{ml0} + \frac{T_l}{K}. \tag{28}$$

Summing up horizontal distances provides the relationship,

$$L_{chain} - S_{up} + X_r + L_{ml}\cos(\phi) = X_0 + \eta_1. \tag{29}$$

Current and Wave Forcing

Current is taken to be constant in time and uniform with depth. Waves may be specified as single frequency waves and represented by linear wave theory. Frequency at the platform is modified by advection of the wave field at the current velocity and referred to as the encounter frequency.

Random seas may also be simulated using the random phase approach. Surface elevation is taken to be a superposition of single frequency contributions, each having a random phase and an amplitude consistent with a specified spectral density. For example, the Brettschneider (1963) spectrum S may be used, for which

$$S = \frac{5}{16}\frac{H_{\frac{1}{3}}^2}{f_{pk}}\left(\frac{\sigma}{\sigma_{pk}}\right)^{-5} exp\left(-\frac{5}{4}\left(\frac{\sigma}{\sigma_{pk}}\right)^{-4}\right) \tag{30}$$

where $H_{1/3}$ is significant wave height, f_{pk} is peak frequency (Hz), and σ_{pk} is radian peak frequency (radians/s).

Numerical Solution

The equations of motion were solved in the time domain using a "marching solution" approach implemented in a MATLAB program. At each time step, the system of nonlinear algebraic equations, including all mooring equations, was solved iteratively, and the dynamic equations used to extrapolate to the next time step. The procedure began using initial conditions for the platform's three degrees of freedom and their derivatives (i.e., the initial position and velocity in three degrees of freedom).

Model Application and Validation

The model was applied to UNH's 10.7-m (35-feet) decked, twin-hulled tidal energy test platform (Rowell, 2013). Damping and acceleration force coefficients were found empirically using a 1/9 scale physical model in tank experiments. The computer model was then used to calculate full-scale mooring loads, turbine forces and platform motion in preparation for a full-scale test of a horizontal axis tidal turbine in Muskeget Channel, which runs north-south between Martha's Vineyard and Nantucket Island. During the field experiments, wave, current and platform motion were recorded. The field measurements were used to compute RAOs, essentially normalized

amplitudes or frequency responses, for heave, pitch, and surge. The measured RAOs were compared with those calculated using the model.

Added mass and damping coefficients for the platform-turbine system in heave and pitch were obtained by measuring the platform's response to an initial perturbation in still water, referred to as a "free-release test." Free-release testing is a standard procedure for characterizing the dynamic response coefficients for oscillating systems (see, e.g., Palm, 2010).

For heave, when no wave, current, or mooring loads are present, Equation 3 simplifies to

$$\ddot{\eta}_3(m + A_{33}) + B_{33}\dot{\eta}_3 + C_{33}\eta_3 = 0 \tag{31}$$

which describes a harmonic oscillating system. Here, A_{33} is the added mass of the system in heave; B_{33} is the system damping in heave; C_{33}, is $\rho g A_{wp}$; and A_{wp} is waterplane area. The solution to Equation 31, when the platform is released from rest at height A, is

$$\eta_3 = \frac{A}{\cos\phi} e^{\zeta\omega_o t}\cos(\omega_d t - \phi) \tag{32}$$

where $\phi = \tan^{-1}\left(\frac{\zeta\omega_o}{\omega_d}\right)$; $\omega_o = \left(\frac{C_{33}}{m + A_{33}}\right)^{\frac{1}{2}}$ is the undamped natural frequency of the system in heave; $\omega_d = \frac{2\pi}{T_d} = \omega_o\sqrt{1 - \zeta^2}$ is damped natural frequency; T_d is the damped natural period; and $\zeta = \frac{B_{33}}{2\omega_o(m + A_{33})}$ is the damping ratio.

FIGURE 4

Annotated sample free-release test of model 10.7-m (35-feet) platform in heave compared to mathematical model of free-release test. Physical model values were Froude scaled to full size.

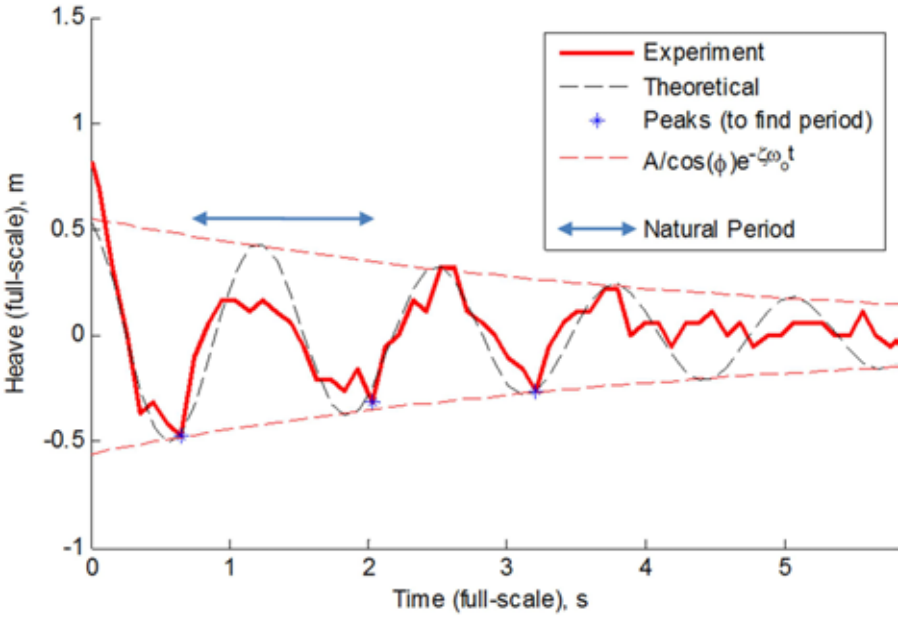

A 1:9 Froude-scaled model of the 10.7-m (35-feet) UNH V1 Tidal Energy Test Platform and the 0.86-m (34-inch) FloDesign tidal turbine was constructed, and its response to heave and pitch perturbations in still water were measured by UNH's Optical Positioning, Instrumentation, and Evaluation (OPIE) system, which is described by Michelin and Stott (1996). Figure 4 shows results from a typical heave free-release test. The average time between negative peaks was taken as the damped natural period T_d. (Zero crossings could have been used.) The solution given by Equation 32 was then fit to two negative peaks in succession to yield the damping ratio ζ. These results were combined with the above parameter definitions to evaluate added mass and damping constants. Six experiments were done, and averaged parameters were used in the mathematical model.

This free-release method was repeated to find the pitch damping and added mass coefficients. The average damped natural period was 1.4 s for heave and 1.0 s for pitch. Drag coefficients (in the surge direction) for both the platform and turbine were found from full-scale physical experiments. The added mass coefficient for the long slender hulls in surge motion was taken to be negligible. For the turbine, added mass in surge was approximated by Equation 21.

The model was then used to predict the dynamic response of the UNH CORE 10.7 m (35 feet) platform to expected conditions in Massachusetts' Muskeget Channel. First, the bow-down inclination angle was calculated using Equation 4 without waves in a steady, predicted tidal current of 2 m/s. It was determined that a surface float needed to be used. Otherwise, the downward pull of the mooring line in

combination with the bow-down moment generated by the 0.86 m (34 inch) diameter FloDesign turbine caused too much reduction in bow freeboard. With the float, steady bow-down inclination was only 0.3°. Wave environments were represented by two single-frequency design waves, one 0.30 m height and 7.5 s period wave for Sea State 2, and one 0.88 m height, 7.5 s period for Sea State 3. It was determined that mooring loads from both sea states could be sustained by an embedment anchor of 227 kg (500 lb) in the expected sand/gravel bottom sediment of the channel. Maximum turbine fluid dynamic forces of 2,500 N and 3,400 N for Sea States 2 and 3, respectively, were acceptable to the turbine manufacturer. Platform motion response predicted for the two sea states indicated that Sea State 2 or less would be highly desirable for field operations, while Sea State 3 or higher would pose operating difficulties possibly endangering crew and equipment.

Ocean Deployment

UNH's 10.7-m (35-feet) tidal energy test platform was used to test the FloDesign hydrokinetic turbine in Muskeget Channel on July 15, 16 and 19, 2012. The energetic environment and the instrumentation onboard the platform made for a good full-scale validation case.

In the full-scale deployment the platform instrumentation included a high-end inertial measurement unit (IMU) provided by the National Renewable Energy Laboratory (NREL), a wave staff mounted on the bow of the platform, load cells, and flow sensors, listed in Table 1. Before deployment, the IMU was calibrated to the greater of 5 cm or 5% for linear position and to ±0.03° for angles smaller than ±5°; the wave staff was calibrated to ±0.4 cm. The wave staff, corrected for platform motion with the IMU, was used to determine the wave forcing spectrum. The IMU was also used to find the platform response spectra, which were used to compute the system RAOs. Load cells were used to measure the mooring loads on the platform.

On each day of testing, the platform was moored on a single-point mooring, shown in Figure 5.

The platform was deployed during two ebb tides and one flood, each on a different day. This mooring system allowed the test platform to align itself with the current, allowing for a wide radius of potential locations. Thus, the water depth at the platform location was recorded on each day of testing so that the wave environment could be modeled accurately.

Platform motion data were recorded continuously at 10 Hz for the duration of the testing and saved in 10 min segments, which were spliced together when processing longer data sets. The wave staff recorded a single file for each day of testing and also sampled at 10 Hz. The vector ADV also recorded a single file for each day of testing, sampling at 32 Hz. The deployment is described in further detail by Rowell (2013) and Dewhurst et al. (2012).

The location of the system's center of gravity (CG) was found using a detailed Solidworks model of the platform-turbine system, accounting for the mass distribution of the crew. Knowing the geometric relation of the IMU to the CG, the platform motion at/about the CG in each degree of freedom was found as

$$\eta_1 = \eta_1^* - R_{IMU3}\sin\eta_5 \tag{33}$$

$$\eta_3 = \eta_3^* - R_{IMU1}\sin\eta_5 \tag{34}$$

where η_1^* and η_3^* are respectively the surge and heave displacement measured at the IMU and R_{IMU1} and R_{IMU3} are respectively the horizontal and vertical components of the vector from the CG to the IMU, shown in Figure 6. Since the system is treated as a rigid body, η_5 needs no correction.

The fluid surface elevation time series was found by correcting the elevation measured by the wave staff with the platform displacement as measured by the IMU. The vertical

TABLE 1

Ocean deployment instrumentation.

Instrument	Model	Manufacturer
Wave Staff	OSSI-010-002E	Ocean Sensor Systems
Acoustic Doppler Velocimeter (ADV)	Vector Cable Probe Standard	Nortek USA
Inertial Motion Unit (IMU)	402225 DMS 3	Teledyne TSS
Load Cells	SS 20000	Sensing Systems

FIGURE 5

Mooring system for ocean deployment.

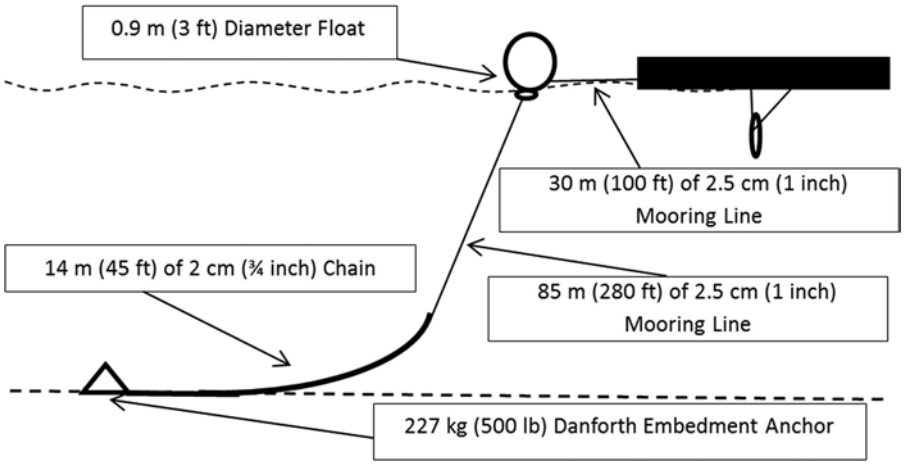

FIGURE 6

UNH CORE 10.7-m (35-feet) platform with instrumentation.

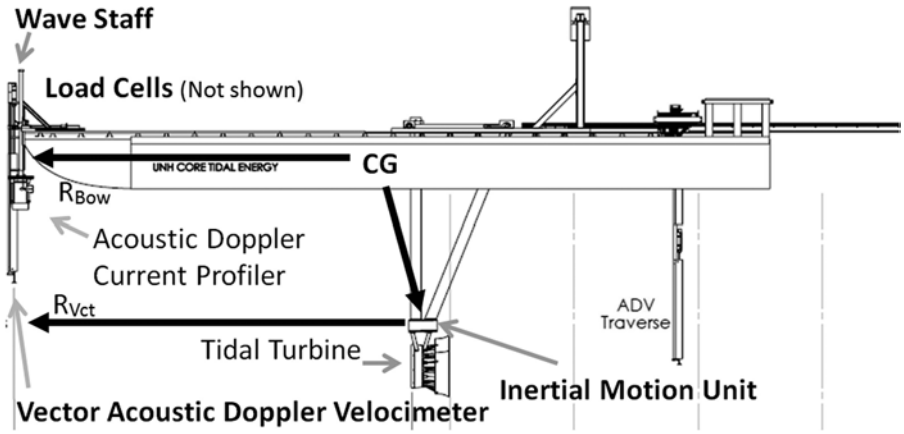

position of the platform bow (on which the wave staff was mounted) was calculated as

$$\eta_{bow3} = \eta_3 + \sin(\eta_5) R_{Bow1} \qquad (35)$$

The wave spectrum was then computed as the power spectral density of the corrected surface elevation time series, ζ_{bow3}, using a Hanning window and ensemble averaging in 5-min ensembles and band averaging over five adjacent Fourier frequencies, as described by, for example, Bendat and Piersol (2010). The power spectral density of the platform motion in each degree of freedom was computed using the same method as for the wave spectrum. The RAO in each degree of freedom was then computed as shown in Table 2. A spectral approach was used because forcing and response were random. Essentially, surge was normalized by horizontal motion of wave forcing at the surface, heave was normalized by the wave amplitude, and pitch was normalized by wave slope.

After the full-scale ocean deployment, the model was applied using two different wave forcing methods—single frequency waves spanning the field spectrum and random seas having the same spectra. For the single frequency waves, model wave height was chosen to match the measured sea significant wave height. Model RAOs were calculated by normalizing heave, pitch, and surge amplitudes by surface wave amplitude for heave and surge and surface wave slope for pitch (see Table 2). For the random sea forcing, the input wave spectrum was specified to match the measured spectrum for that comparison case. The random phase method was then used to compute the wave surface elevation time

TABLE 2

RAO definitions.

Mode of Motion	Wave Type	
	Single Frequency	Random
Surge	$\frac{(\eta_{1max} - \eta_{1min})}{H}$	$\sqrt{\frac{S_{platform1}}{S_\zeta}}$
Heave	$\frac{(\eta_{3max} - \eta_{3min})}{H}$	$\sqrt{\frac{S_{platform3}}{S_\zeta}}$
Pitch	$\frac{(\eta_{5max} - \eta_{5min})}{Hk}$	$\sqrt{\frac{S_{platform5}}{k^2 S_\zeta}}$

series used to drive the mathematical model. Model predictions for heave, pitch, and surge time series were then processed using the same steps as for the field data.

Figure 7 compares measured RAOs with single frequency and random sea model predictions under following sea conditions (current and wave direction opposed). Head sea conditions (current and wave direction the same) are shown in Figure 8. For both the Figure 7 and Figure 8 situations, crew member positions were fixed during the experiment, while in Figure 9 the four-member crew was allowed to move freely on deck.

In general, the Figures 7, 8, and 9 comparisons indicate that the model replicates response magnitudes and frequency dependent trends. To provide a quantitative comparison, the model skill was computed for each case according to

$$S = 1 - (nRMS)^2 \tag{36}$$

where *nRMS* is the root mean square error between observations and model results normalized by root mean square of the observations. The results of the skill calculation are shown in Table 3.

Results for surge and heave prediction are very good for all environments considered ($S \geq 0.85$). Pitch response predicted by the model for following seas, and the Figure 8 head sea case is also good. For the Figure 9 head sea case, however, the model overpredicts pitch response, leading to a low skill value. In this case, crew position was not restricted during the experiment.

To characterize model sensitivity to added mass and damping coefficients determined in the scale model free-release tests, the percent change in RAO values, at a midrange wave frequency of 1.2 rad/s, was calculated for the following sea (Figure 7) case when heave calibrated coefficients were varied by ±20%. The results are shown in Table 4.

Comparisons indicated that the model is relatively insensitive to parameter changes. For the experimental conditions, total normal fluid force on the line was less than 15% of line

FIGURE 8

Current: 1.9 m/s, significant wave height: 0.5 m, head seas. Ocean data: 4 ensembles, 5 bands. 95% confidence intervals, based on *F*-distribution, are shown at every third banded frequency. Average of top 5% of predicted force peaks was 431 lb; average of top 5% of measured force peaks was 323 lb.

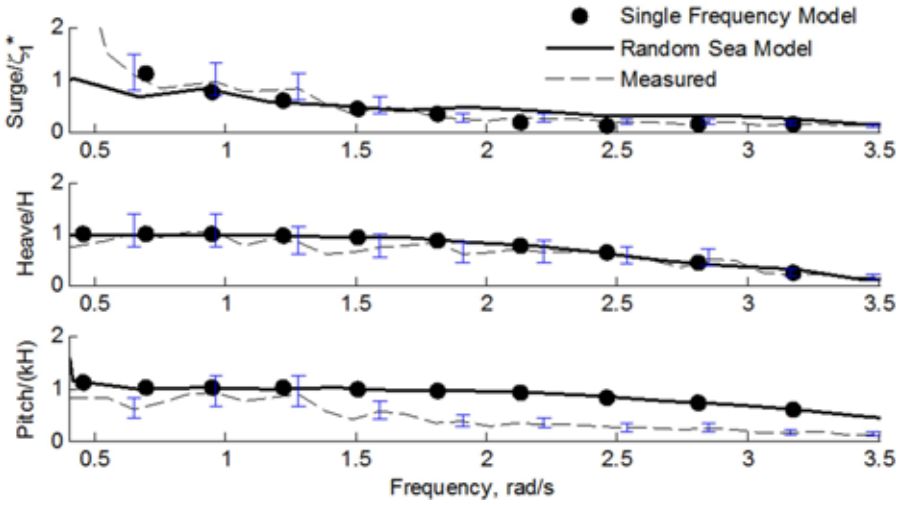

FIGURE 7

Current: 1.5 m/s, significant wave height: 1.0 m, following seas. Ocean data: 4 ensembles, 5 bands. 95% confidence intervals, based on *F*-distribution, are shown at every other banded frequency. Average of top 5% of predicted force peaks was 591 lb; average of top 5% of measured force peaks was 557 lb.

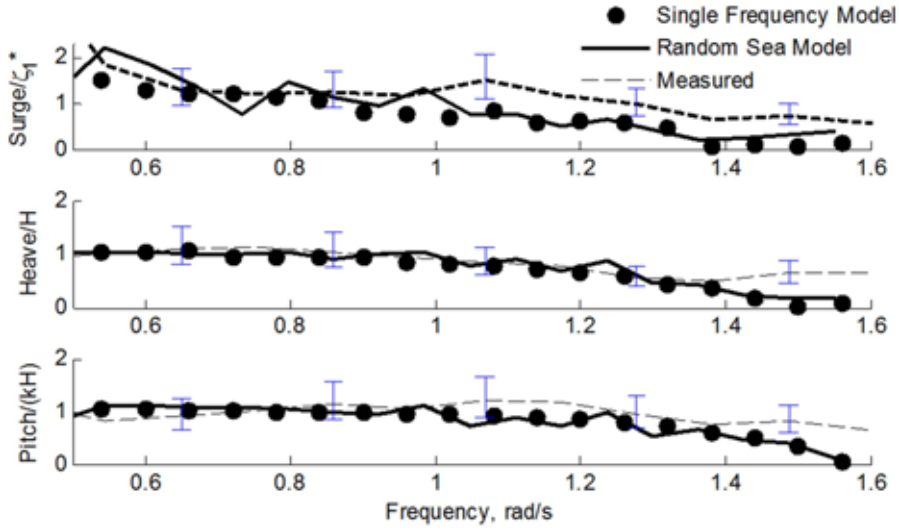

FIGURE 9

Current: 1.5 m/s, significant wave height: 0.5 m, head seas. Ocean data: 2 ensembles, 5 bands. 95% confidence intervals, based on *F*-distribution, are shown at every third banded frequency. Average of top 5% of predicted force peaks was 289 lb; average of top 5% of measured force peaks was 261 lb.

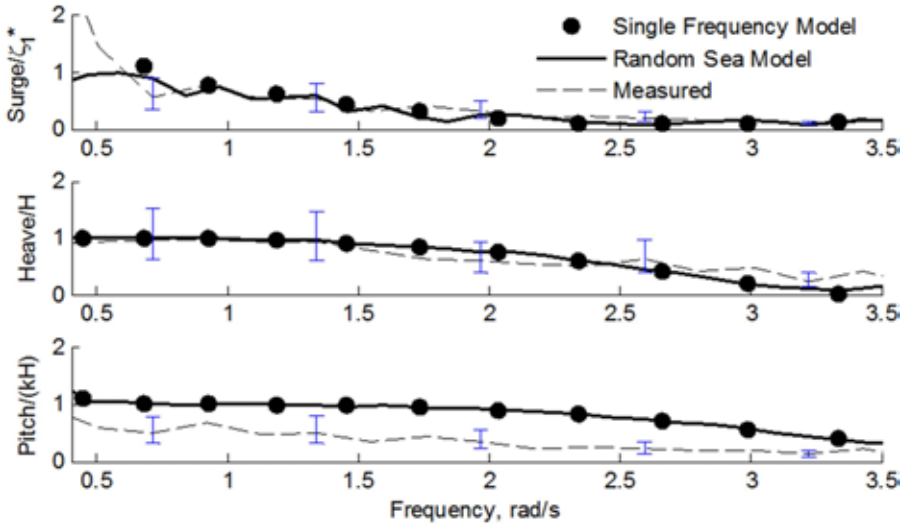

tension, so neglecting drag force on the mooring system did not introduce significant error.

Discussion

The generally favorable comparison between predicted and observed RAOs indicates that the mathematical model captures the essential physics governing floating platforms in current and waves. For the exception of pitch when mass positions were not constrained, the model prediction is conservative, which is normally acceptable for design purposes. It should be noted that the heave and pitch RAOs do not exhibit a "resonance" at the natural frequencies identified in the free-release tests. This is because the frequencies are high enough that the wavelengths are short compared to waterline lengths and the net forcing effect is negligible (see Equations 6, 9, 15). The long, light hulls used are, therefore, optimal from this standpoint. The model has also been demonstrated to be an effective and useful design tool in preparation for field experiments in which the platform supports the testing of a tidal turbine.

For commercial platforms and for larger test platforms to be used for extended deployments, the model capabilities should be more fully utilized. For example, a 29-m floating platform is presently being developed for use in Muskeget Channel (Dewhurst, 2013, Swift et al., 2013). In this application, steady bow-down inclination and mooring loads are calculated as in the preparation for the Summer 2012 field deployment. In addition, the

TABLE 3

Model skill.

	Surge, Single Frequency	Surge, Random	Heave, Single Frequency	Heave, Random	Pitch, Single Frequency	Pitch, Random
Following seas (Figure 7)	0.85	0.88	0.94	0.96	0.95	0.93
Head seas A (Figure 8)	0.97	0.85	0.97	0.97	0.83	0.83
Head seas B (Figure 9)	0.90	0.96	1.00	1.00	0.16	0.19

TABLE 4

Sensitivity of sea-keeping model.

	Heave added mass increased by 20%	Heave added mass decreased by 20%	Heave damping increased by 20%	Heave damping decreased by 20%
Surge RAO, % change	0%	0%	0%	0%
Heave RAO, % change	–1%	0%	0%	1%
Pitch RAO, % change	0%	0%	0%	0%

model is forced by random seas inferred for the site using long-term wave statistics compiled at the nearby Martha's Vineyard Coastal Observatory. Bow clearance is predicted using platform motion time series to calculate bow height from which a surface elevation time series is subtracted. Percent time for which there is no wave slamming or water on deck can then be found. Similarly, vertical accelerations can be computed, allowing operating times to be determined for which various sea-sickness criteria are satisfied. Thus, this computer simulation is expected to be a practical design tool able to answer many important design questions regarding floating platform dynamics.

Acknowledgments

The authors gratefully acknowledge the University of Massachusetts and the Department of Energy for their financial support. The authors thank FloDesign, Inc., for entrusting UNH-CORE with the deployment of their hydrokinetic turbine. The loan of instruments by the National Renewable Energy Laboratory, Boulder, Colorado, for the Summer 2012 deployment is also very much appreciated. In addition, the authors thank Dr. Thomas Lippmann for his helpful discussions regarding spectral analysis and data processing.

Corresponding author:

Tobias Dewhurst
Center for Ocean Renewable Energy
University of New Hampshire
24 Colovos Rd.
Durham, NH, 03824
Email: toq4@unh.edu

References

Bahaj, A., Molland, A., Chaplin, J., & Batten, W. 2006. Power and thrust measurements of marine current turbines under various hydrodynamic flow conditions in a cavitation tunnel and a towing tank. Renew Energ. 32(3):407-26.

Bendat, J.S., & Piersol, A.G. 2010. Random Data: Analysis and Measurement Procedures. 4 ed. New York: John Wiley & Sons. 640 pp.

Berteaux, H.O. 1991. Coastal and Oceanic Buoy Engineering. Woods Hole, MA: Author. 285 pp.

Bretschneider, C.L. 1963. A one-dimensional gravity wave spectrum. Ocean Wave Spectra. Prentice-Hall Inc., New York. 41-6.

Byrne, J. 2011. Development of a Tidal Energy Test Facility. In: 3rd Annual New England Marine Renewable Energy Center Technical Conference. Cambridge, MA.

Byrne, J. 2013. Design of a floating platform for testing hydrokinetic turbines. Master's thesis. Durham: University of New Hampshire. In preparation.

Dewhurst, T., Rowell, M., DeCew, J., Baldwin, K., Swift, M.R., & Wosnik, M. 2012. Turbulent inflow and wake of a marine hydrokinetic turbine, including effects of wave motion. Bull Amer Phys Soc. 57(17):146.

Dewhurst, T. 2013. Design of a tidal energy test platform for the Muskeget Channel. Master's thesis. Durham: University of New Hampshire. 180 pp.

Faltinsen, O.M. 1990. Sea Loads on Ships and Offshore Structures. Cambridge: Cambridge University Press. 328 pp.

Francis, M., & Hamilton, M. 2007. SRTT Floating Tidal Turbine Production Design Study with Independent Verification. Submitted to Department for Business: Enterprise and Regulatory Reform.

Hewitt, R. 2010. Early tidal power test in Eastport called a success. Bangor Daily News, Bangor, ME. A4.

Korvin-Kroukovsky, B., & Jacobs, W. 1957. Pitching and heaving motions of a ship in regular waves. Trans Soc Naval Arch Mar Eng. 57:590-632.

Lamb, H. 1932. Hydrodynamics. 6 ed. Cambridge: Cambridge University Press. 738 pp.

Michelin, D., & Stott, S. 1996. Optical Positioning, Instrumentation and Evaluation. Durham: University of New Hampshire. 85 pp.

Palm, W.J. 2010. System Dynamics. 4 ed. New York: McGraw Hill. 834 pp.

Rowell, M. 2013. A scaled approach to testing a second-generation hydrokinetic turbine. Masters thesis. Durham: University of New Hampshire. 172 pp.

Salvesen, N., Tuck, E.O., & Faltinsen, O.M. 1970. Ship Motions and Sea Loads. Trans Soc Naval Arch Mar Eng. 78:250-87.

Sariöz, K., & Narli, E. 2005. Effect of criteria on seakeeping performance assessment. Ocean Eng. 32:1161-73. http://dx.doi.org/10.1016/j.oceaneng.2004.12.006.

St. Denis, M., & Pierson, W. 1953. On the motion of ships in confused seas. Trans Soc Naval Arch Mar Eng. 61. Jersey City, NJ.

Swift, M.R., Baldwin, K., Wosnik, M., Celikkol, B., Tuskrov, I, Dewhurst, T, & Byrne, J. 2013. Muskeget Channel tidal energy test facility. Final report submitted to the University of Massachusetts at Dartmouth. University of New Hampshire, Durham. 108 pp.

The Society of Naval Architects and Marine Engineers. 1988. Principles of Naval Architecture, Second Revision. Jersey City, NJ. 429 pp.

Verdant Power. 2005. Amesbury tidal energy project. Final report submitted to the Massachusetts Technology Collaborative. Boston, MA. 178 pp.